Supporting Information

High-χ Diblock Copolymers Containing Poly(vinylpyridine-N-oxide) Segments

Polyxeni P. Angelopoulou,[a,b] Logan T. Kearney,[c] Jong K. Keum,[a,d] Liam Collins,[a] Rajeev Kumar,[a] Georgios Sakellariou,[b] Rigoberto C. Advincula,[a] Jimmy W. Mays,*[e] Kunlun Hong *[a]

[a] Center for Nanophase Materials Sciences, Oak Ridge National Laboratory, Oak Ridge, TN 37831, USA

[b] Department of Chemistry, National and Kapodistrian University of Athens, Athens, 15771, Greece

[c] Chemical Sciences Division, Oak Ridge National Laboratory, Oak Ridge, TN 37831, USA

[d] Neutron Scattering Division, Oak Ridge National Laboratory, Oak Ridge, TN 37831, USA

[e] Department of Chemistry, The University of Tennessee, Knoxville TN 37996, USA

Synthesis of PS-*b*-P2VP diblock copolymers The linear precursor PS-*b*-P2VP block copolymers were anionically polymerized by sequential addition of monomers (Scheme S1).

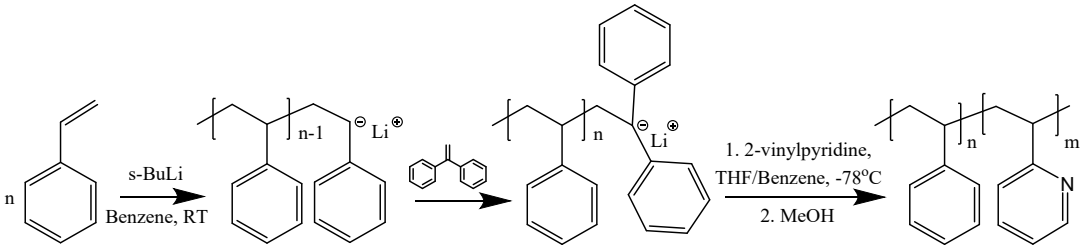

Scheme S1. Synthesis of PS-*b*-P2VP diblock copolymer

In a typical synthetic procedure, as for example for sample PS_{34}-*b*-$P2VP_{27}$, styrene was polymerized under high-vacuum using break-seal techniques with *sec*-BuLi as the initiator. The polymerization took place in a tailor-made all-glass apparatus equipped with ampoules containing desired amounts of *sec*-BuLi (0.43 mmol, 1.53 mL solution in hexane) and styrene (1.7 g, 16.32 mmol) depending on the target molecular weight of the polystyrene, while an empty ampoule for the "living" polymer to be collected in, was, also, used. The ampoules with the monomer and the initiator were introduced by smashing the respective break-seals. The monomer and the initiator were added in the polymerization reaction apparatus which contained purified benzene (17 mL) as the solvent. The solution spontaneously obtained a red-orange color. The polymerization was left to proceed for 20 hours at room temperature. After another 20 hours, an ampoule containing DPE

(0.71 mmol, 1.4 mL solution in hexane) was smashed and the solution turned dark red. An aliquot of the macroinitiator was collected and characterized by SEC after termination with methanol.

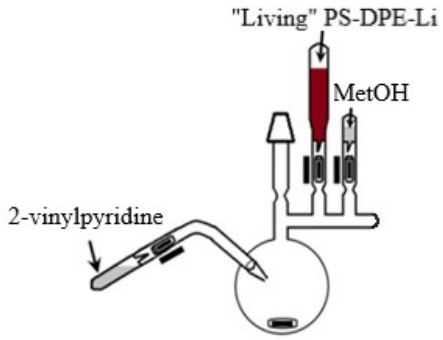

Figure S1. Apparatus for the anionic polymerization of P2VP from "living" PS-DPE^{-}Li^{+}.

The "living" PS-DPE^{-}Li^{+} solution was then integrated to another all-glass polymerization apparatus for the synthesis of P2VP. (Fig. S1)

The apparatus was degassed in the high-vacuum line, and purified THF was distilled. The apparatus was purged according to the anionic polymerization standards, THF was distilled from the purge section flask to the polymerization reactor and the purge section was then heat sealed.[1,2] The polymerization flask, containing THF (40ml) was chilled to -78 °C with dry-ice/isopropanol bath and the macroinitiator (PSLi, 0.49 mmol, 18 mL solution) was added. The second monomer, 2-vinylpyridine (1.7 g, 16.2 mmol) was distilled into the flask under rigorous stirring over 15 minutes. The red color of the initiator turned orange due to the P2VP "living" chain ends. The solution was left at -78 °C, under continuous stirring for 3 hours to ensure completion of the polymerization. Finally, degassed MeOH was added to terminate the polymerization. Precipitation in hexane followed and after filtration and drying, a white powder was obtained. dPS$_{77}$-*b*-P2VP$_{76}$ was synthesized on a similar manner.

Synthesis of PS-*b*-P4VP diblock copolymers The linear precursor PS-*b*-P4VP block copolymers were anionicly polymerized by sequential addition of monomers (Scheme S2). Since P4VP is insoluble in benzene, both styrene and 4-vinylpyridine were polymerized in THF, in low concentration and in the absence of benzene. In this case, as well, anionic polymerization took place in a tailor-made all-glass reactor.

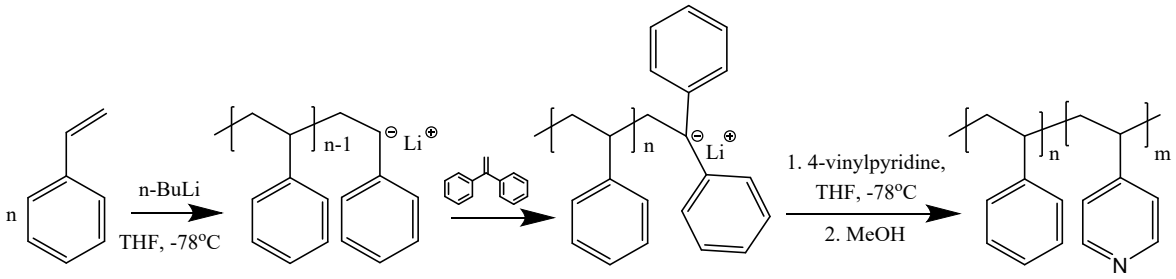

Scheme S2. Synthesis of PS-*b*-P4VP diblock copolymer

In a typical procedure, as for example for PS_{45}-*b*-$P4VP_{12}$, firstly, the apparatus (Fig. S2) was attached to the high-vacuum line and degassed.

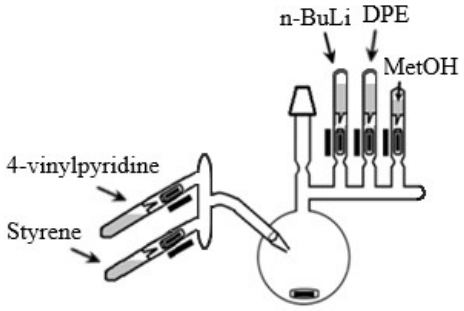

Figure S2. Apparatus for the anionic polymerization of PS-*b*-P4VP

The ampoule with *n*-BuLi (0.49 mmol, 1.88 ml solution in hexane) was smashed, and the non-polar hexane was removed in the high-vacuum line. Pure THF was distilled in the flask of the reactor that was held at -78 °C and the apparatus was heat sealed and detached from the high-vacuum line. *n*-BuLi was preferred over *sec*-BuLi due to lower reactivity with THF.[1] The amount of THF added (100 ml) was relatively high (4VP concentration 1% w/v). Then, the flask was chilled to -78 °C with dry ice/isopropanol bath, the ampoule of the first monomer, styrene (2.7 g, 25.92 mmol), was smashed and the solution became instantly orange. Styrene was allowed to distill over 15 min and the polymerization of the first block was left to proceed for 2 hours under vigorous stirring. After this time, the ampoule containing DPE (0.98 mmol, 1.95 ml solution in hexane) was smashed, the solution became red, and the reaction medium was let at -78 °C for 1 hour. An aliquot of the macroinitiator PS-DPE$^-$Li$^+$ was not isolated and characterized because of concerns about pyrolysis of THF. Afterwards, the ampoule of the second monomer, 4-vinylpyridine (0.98 g, 9.32 mmol), was smashed; the solution took an orange color, and the monomer was allowed to distill in the reactor over 30 minutes, upon which time the polymerization was allowed to proceed for at least 5 hours before it was terminated with degassed MeOH. Precipitation in hexane followed and

after filtration and drying, a white powder was obtained. In the case of PS_{34}-b-$P4VP_{27}$, fractionation in chloroform/hexane was used to purify the copolymer from low molecular weight polymer impurities.

Solubility Solubility tests on homopolymers P2VPNO and P4VPNO took place. These homopolymers were extremely soluble in water. It was, also, noticed that in polar solvents (e.g., DMF, or CH_3CN) they could not easily dissolve. P2VPNO appeared to be less polar than P4VPNO, as was expected since P2VP is less polar than P4VP. The fact that P4VPNO was insoluble in certain polar solvents (e.g., MeOH) in which P2VPNO was more soluble, highlights the higher polarity of P4VPNO as compared to P2VPNO and its very high polarity overall. Since a vast difference in the polarity (i.e. vast difference in solubility parameter, δ) between the blocks of a block copolymer is associated with a high Flory-Huggins, χ, parameter; PS-*b*-P4VPNO was expected to have a higher χ parameter compared to PS-*b*-P2VPNO; while PS-*b*-P2VPNO should, also, demonstrate very high immiscibility as compared to most block copolymers.[3–5] It should be noted that PS-*b*-P4VP already has a very high χ parameter, χ=0.4, while PS-*b*-P2VP has a relatively high χ parameter χ=0.11 (150^{o}C).[6] For the solubility tests very dilute solutions on the order of 0.1% w/v were used.

Table S1. Solubility of P2VPNO and P4VPNO.

	P2VPNO			**P4VPNO**		
	Soluble	Insoluble	Suspension	Soluble	Insoluble	Suspension
Water	●			●		
Trifluoroethanol	●			●		
$CHCl_3$			●		●	
MeOH	●					●
p-Dioxane: Water	●			●		
Acetone: Water	●			●		
THF		●			●	
p-dioxane		●			●	
IsoPrOH	●				●	
DMSO		●			●	
DMF			●		●	
CH_3CN		●			●	
DCM			●		●	
Pyridine		●			●	
1,2-dichlorobenzene			●		●	

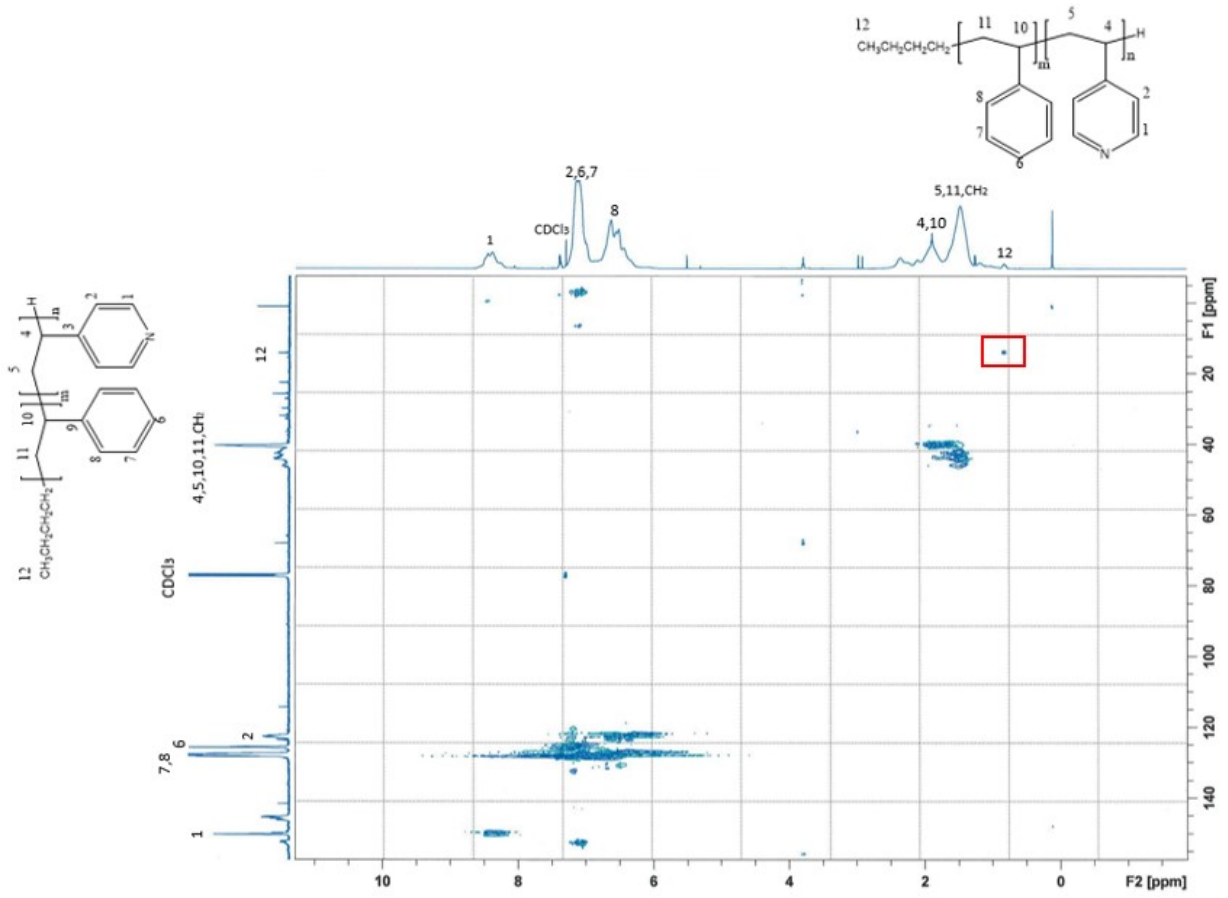

Figure S3. Heteronuclear single quantum coherence (HSQC) ^{1}H-^{13}C spectrum of PS_{45}-*b*-$P4VP_{12}$ in $CDCl_3$. The peak at 0.88ppm in ^{1}H-NMR is associated with the methyl protons of *n*-BuLi.

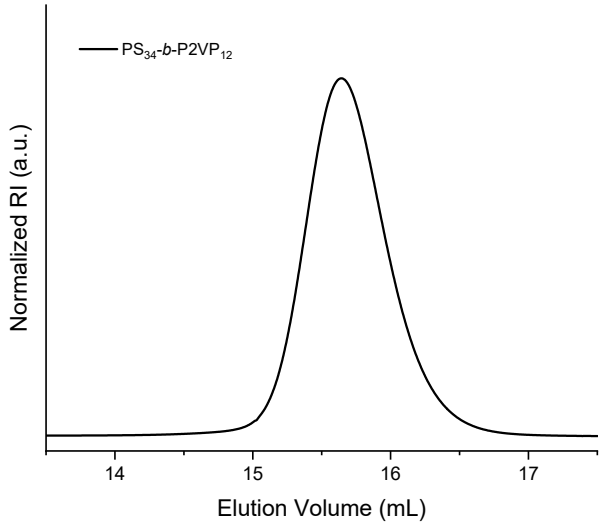

Figure S4. SEC chromatogram of PS_{34}-*b*-$P2VP_{12}$ diblock copolymer

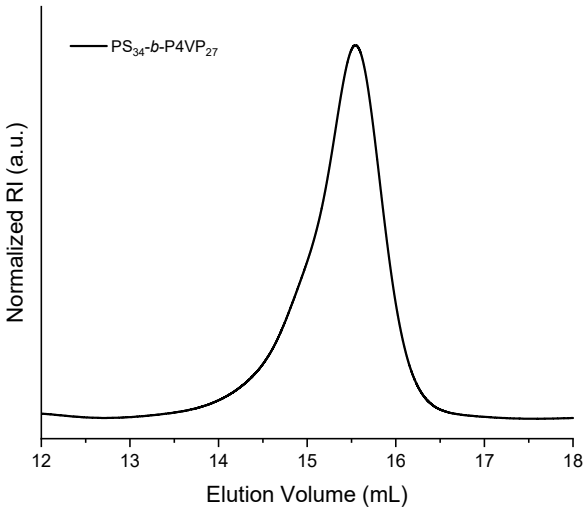

Figure S5. SEC chromatogram of PS_{34}-*b*-$P4VP_{27}$ diblock copolymer

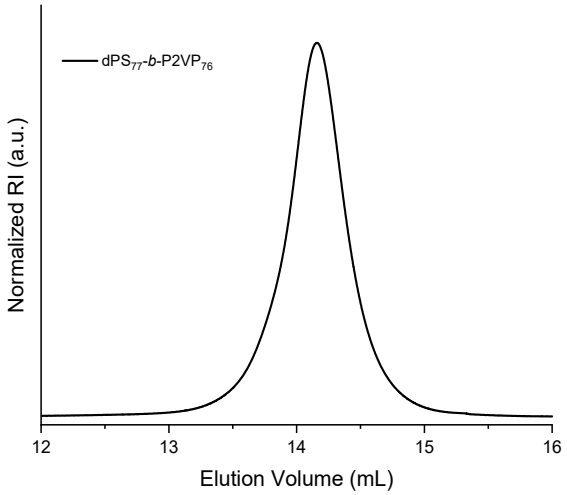

Figure S6. SEC chromatogram of dPS_{77}-*b*-$P2VP_{76}$ diblock copolymer

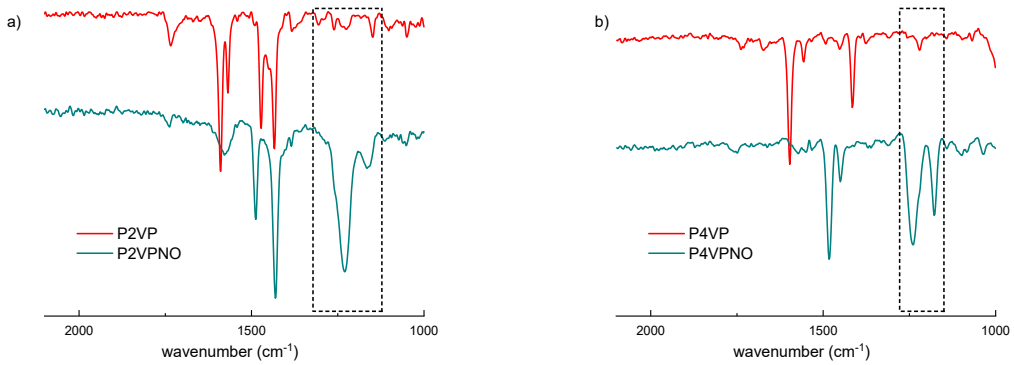

Figure S7. a) ATR-FTIR data of P2VP (red) P2VPNO (dark green). $M_{n,P2VP}$=31.5K, $M_{n,P2VPNO}$=36.3K, b) ATR-FTIR data of P4VP (red) P4VPNO (dark green). $M_{n,P4VP}$=2.9K, $M_{n,P4VPNO}$=3.3K. The bands at 1170 and 1230 cm^{-1} corresponding to oxygen bending vibration and N^{+}-O^{-} stretching vibration of N^{+}-O^{-} are prominent after the oxidation.

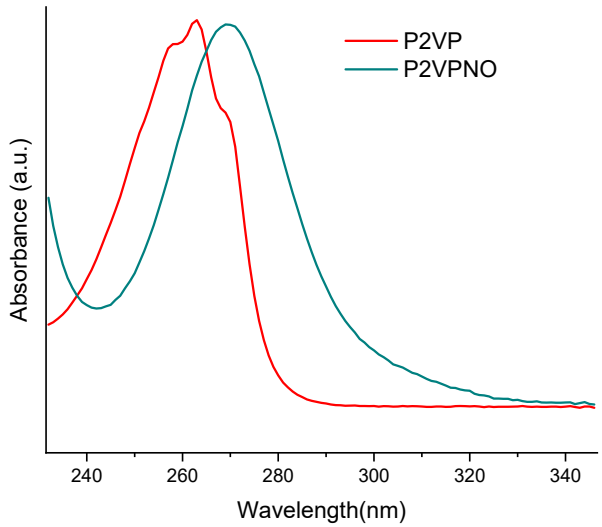

Figure S8. UV-Vis spectra of P2VP (M_n=31.5K) and P2VPNO (M_n=36.3K) in IPA. Upon oxidation the band at λ_{max}=270 nm appears without the prominent shoulders observed before oxidation.

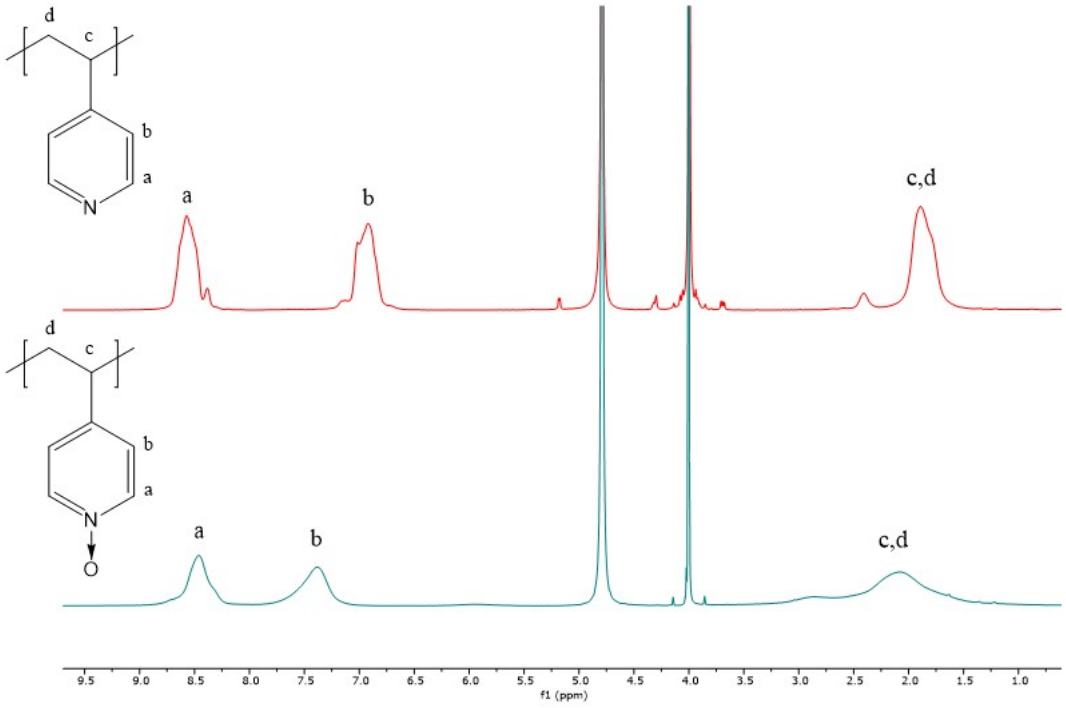

Figure S9. ^{1}H-NMR spectra of P4VP (M_n=68.6K) and P4VPNO (M_n=79.0K) in dioxane-d8/D_2O 70/30 v/v. Upon oxidation the peak associated with the protons of the 2 and 6-positions shifts downfield.

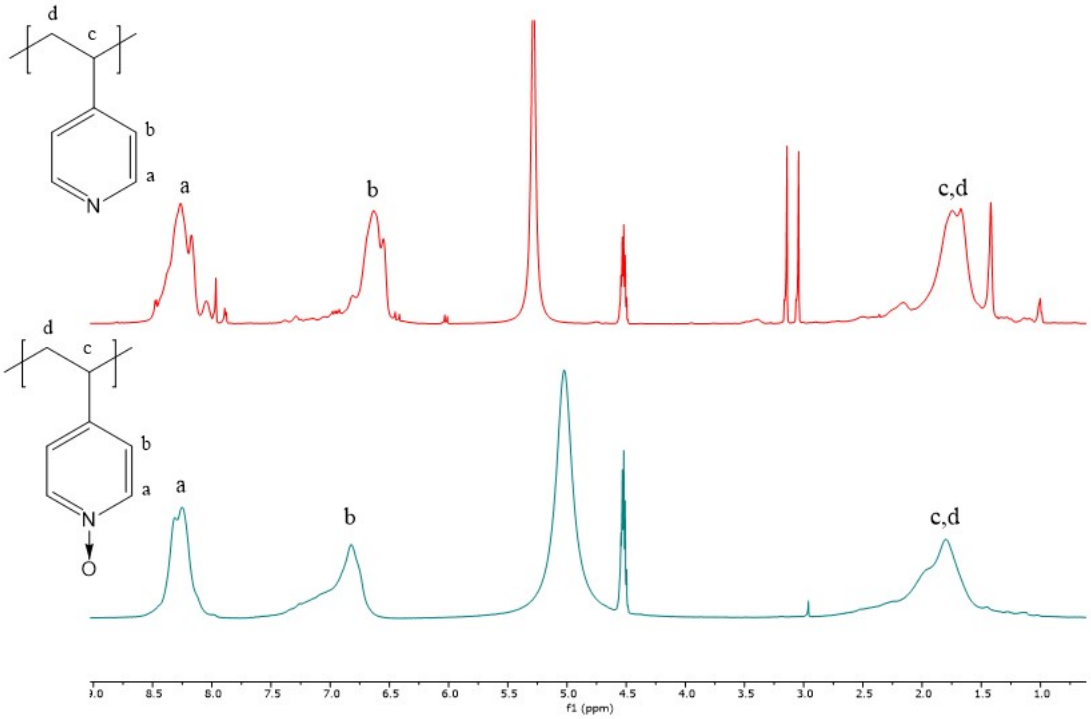

Figure S10. ^{1}H-NMR spectra of P4VP (M_n=2.9K) and P4VPNO (M_n=3.3K) in HFIP-d2. Upon oxidation the peak associated with the protons of the 2 and 6-positions shifts downfield.

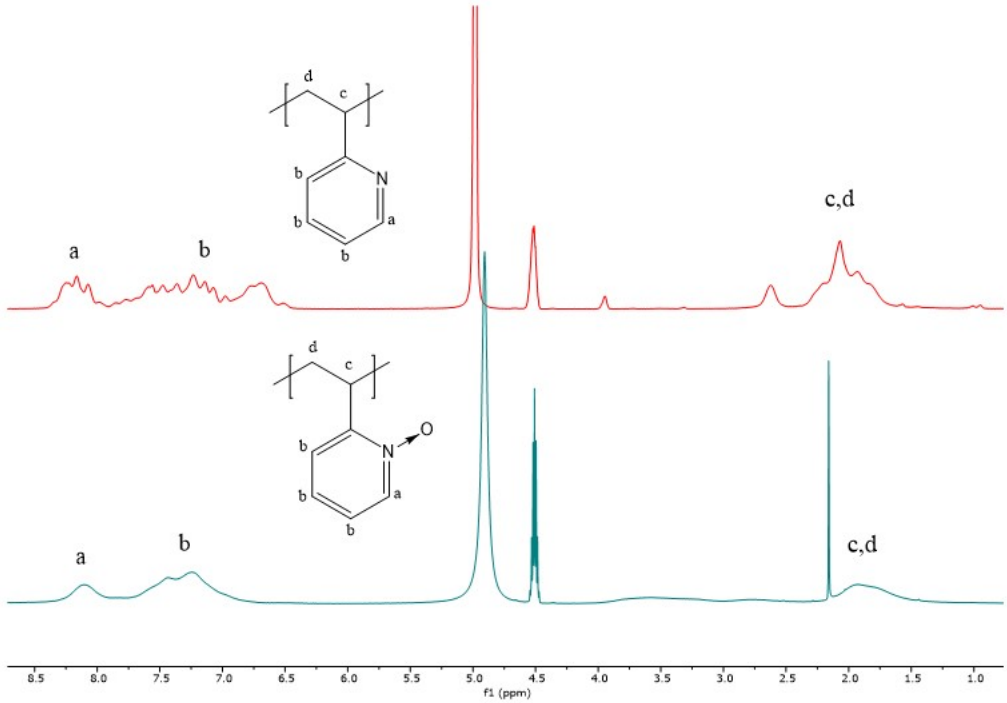

Figure S11. ^{1}H-NMR spectra of P2VP (M_n=31.5K) and P2VPNO (M_n=36.3K) in HFIP-d2. Upon oxidation the peak associated with the protons of the 6-position shifts downfield.

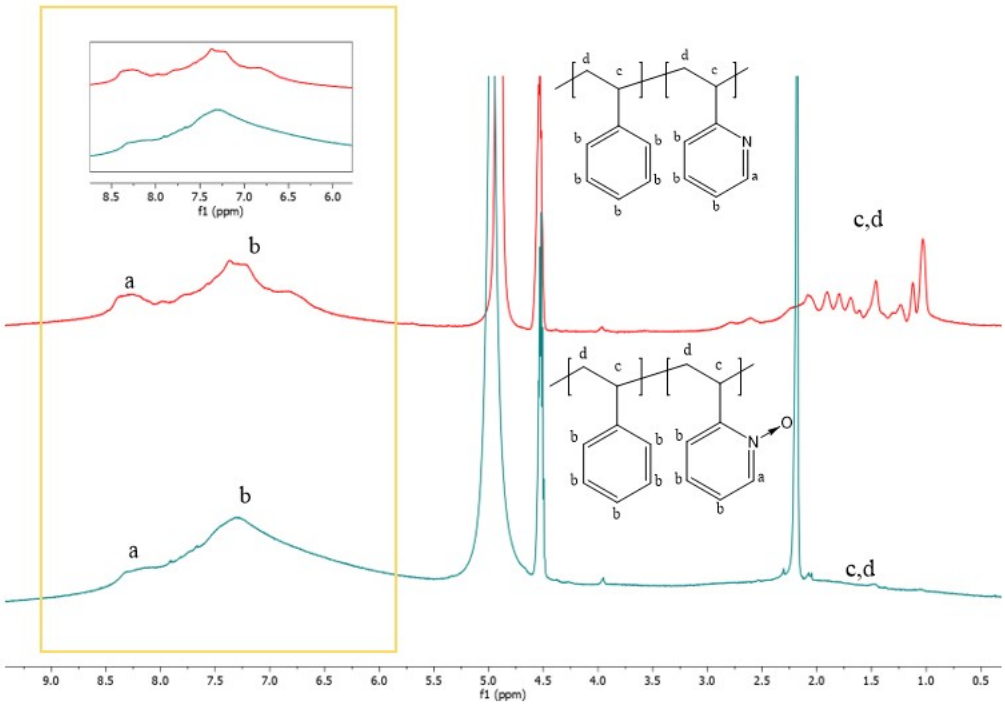

Figure S12. ^{1}H-NMR spectra of PS-*b*-P2VP (M_n=4.8K f_{PS}=0.75) and PS-*b*-P2VPNO in HFIP-d2. Upon oxidation the peak associated with the protons of the 6-position in the P2VP block shifts downfield.

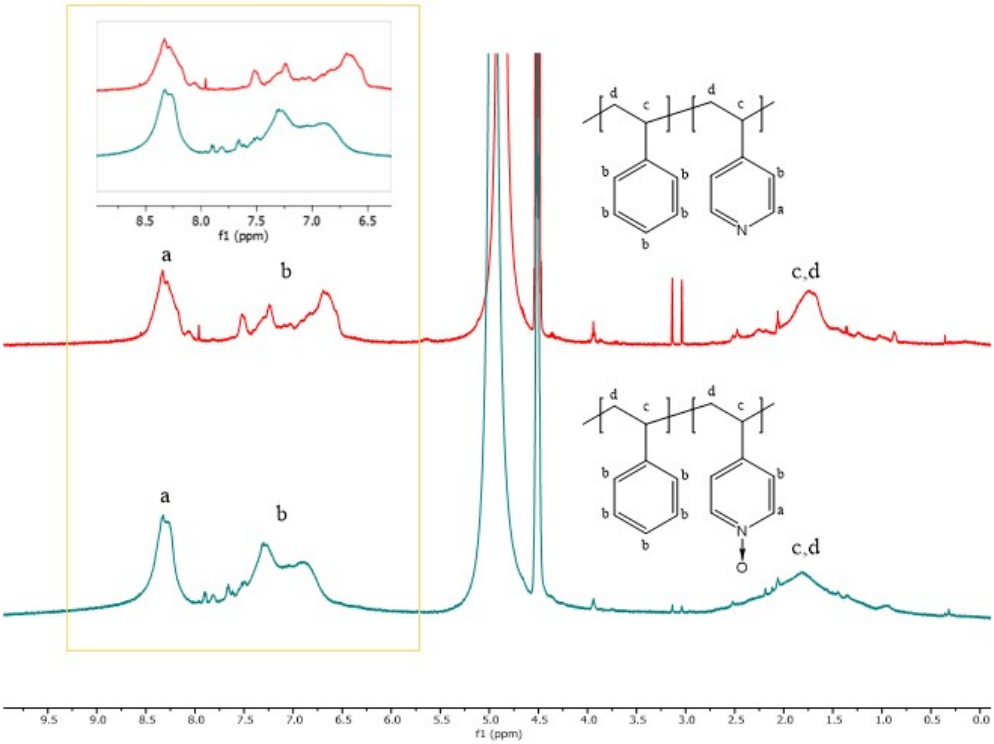

Figure S13. ^{1}H-NMR spectra of PS-*b*-P4VP (M_n=6.0K f_{PS}=0.79) and PS-*b*-P4VPNO in HFIP-d2. Upon oxidation the peak associated with the protons of the 2 and 6-positions of the P4VP block shifts downfield.

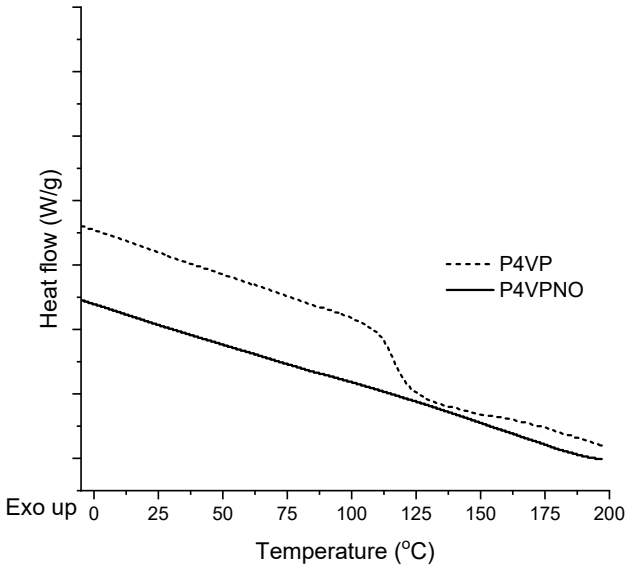

Figure S14. DSC thermograms of precursor P4VP (M_n=17.1K) (dashed line) and final P4VPNO (M_n=19.7K) (solid line) homopolymers

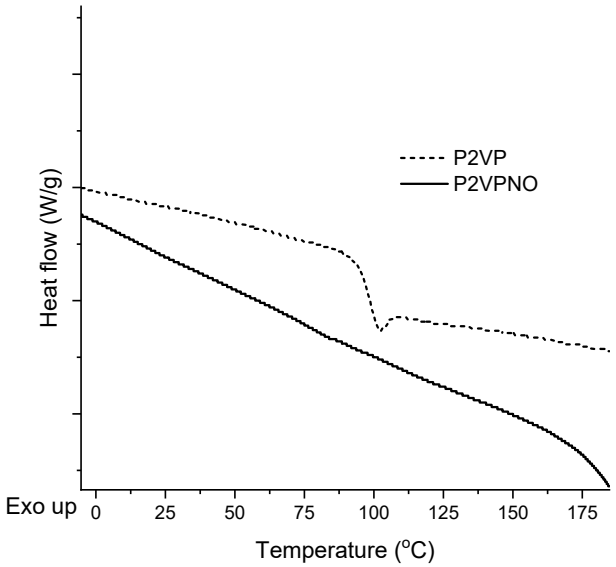

Figure S15. DSC thermograms of precursor P2VP (M_n=31.5K) (dashed line) and final P2VPNO (M_n=36.3K) (solid line) homopolymers

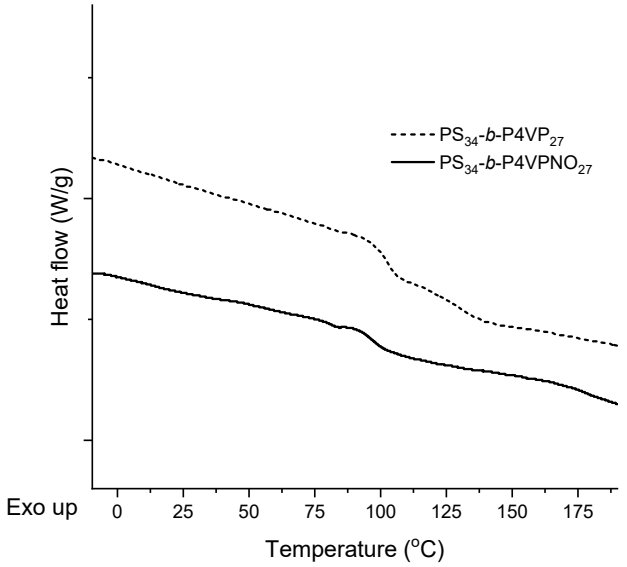

Figure S16. DSC thermograms of precursor PS_{34}-*b*-$P4VP_{27}$ (dashed line) and final PS_{34}-*b*-$P4VPNO_{27}$ (solid line) block copolymers

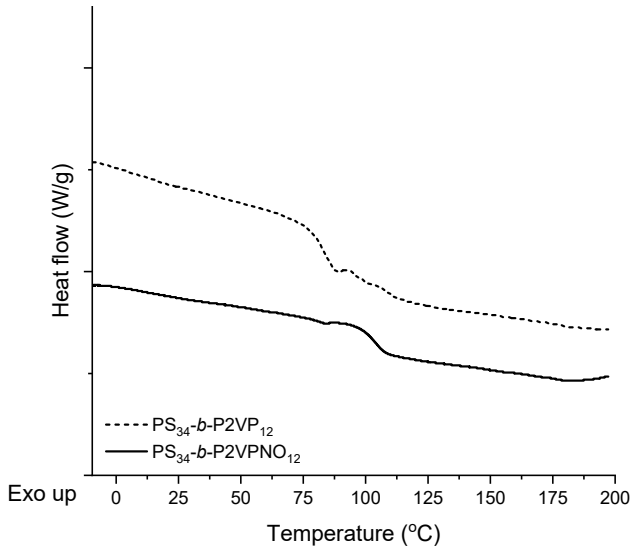

Figure S17. DSC thermograms of precursor PS_{34}-*b*-$P2VP_{12}$ (dashed line) and final PS_{34}-*b*-$P2VPNO_{12}$ (solid line) block copolymers

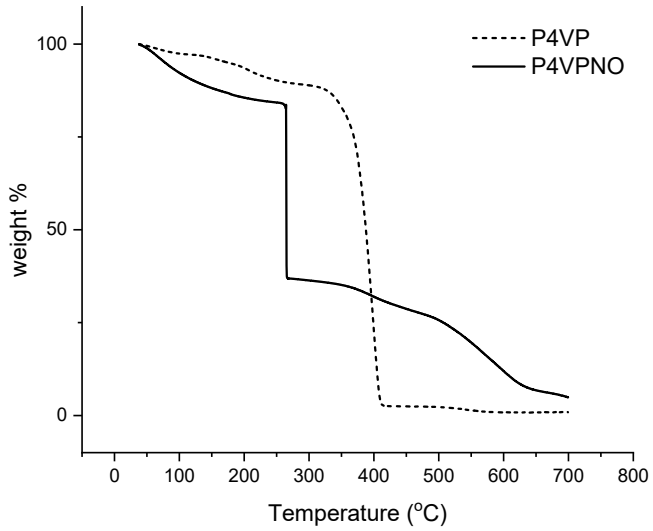

Figure S18. Thermal gravimetric analysis (TGA) curves of P4VP (M_n=17.1K) (dashed line) and P4VPNO (M_n=19.7K) (solid line) homopolymers

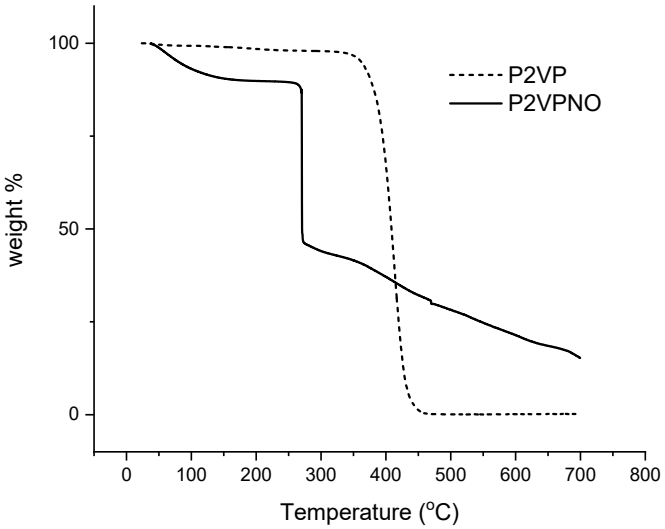

Figure S19. Thermal gravimetric analysis (TGA) curves of P2VP (M_n=31.5K) (dashed line) and P2VPNO (M_n=36.3K) (solid line) homopolymers

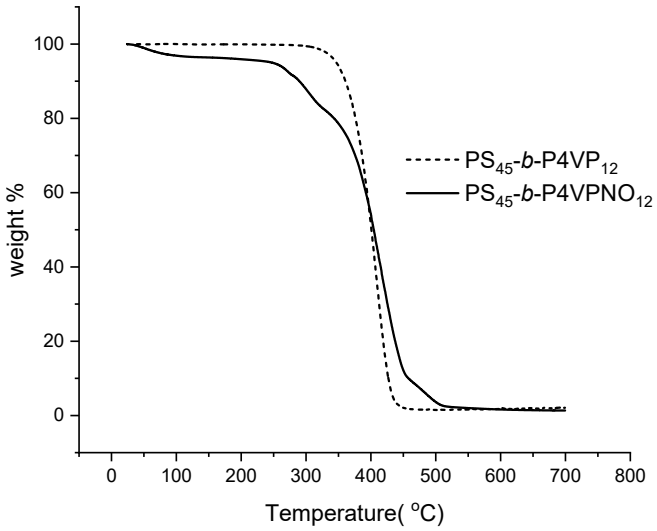

Figure S20. Thermal gravimetric analysis (TGA) curves of precursor PS_{45}-*b*-$P4VP_{12}$ (dashed line) and final PS_{45}-*b*-$P4VPNO_{12}$ (solid line) block copolymers

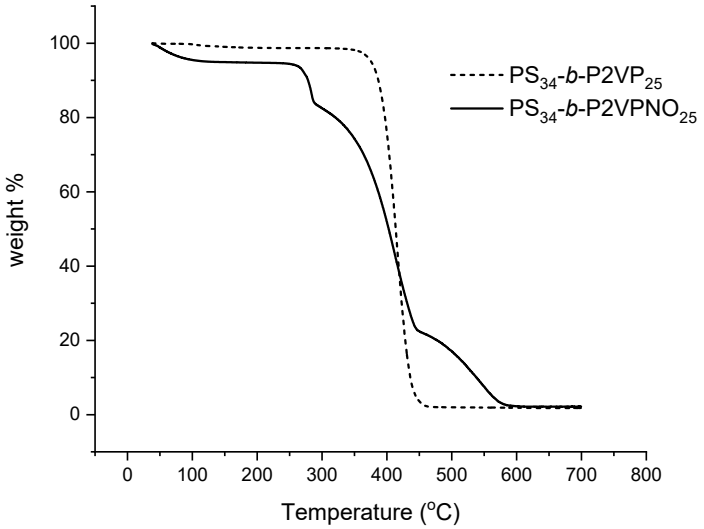

Figure S21. Thermal gravimetric analysis (TGA) curves of precursor PS_{34}-*b*-$P2VP_{25}$ (dashed line) and final PS_{34}-*b*-$P2VPNO_{25}$ (solid line) block copolymers

Degradation investigation

After a degradation investigation upon heating the oxidized homopolymers ($M_{n,P4VPNO}$=19.7K, $M_{n,P2VPNO}$=36.3K) at high Temperatures for short periods of time, and subsequent characterization

by FTIR; it was evident that the oxidized polymers are stable up to 200°C with possible partial degradation/structure deterioration as the temperature increases farther than that. (Fig. S22, S23) In TGA thermograms the T_d onset of the homopolymers appears at ~265°C (Fig. S14, 15), but due to bound water the evaluation of an exact degradation onset from TGA is avoided. The sufficient amount of bound water is, also, indicative of the hygroscopic nature of the oxidized poly(vinylpyridine)s.[7,8]

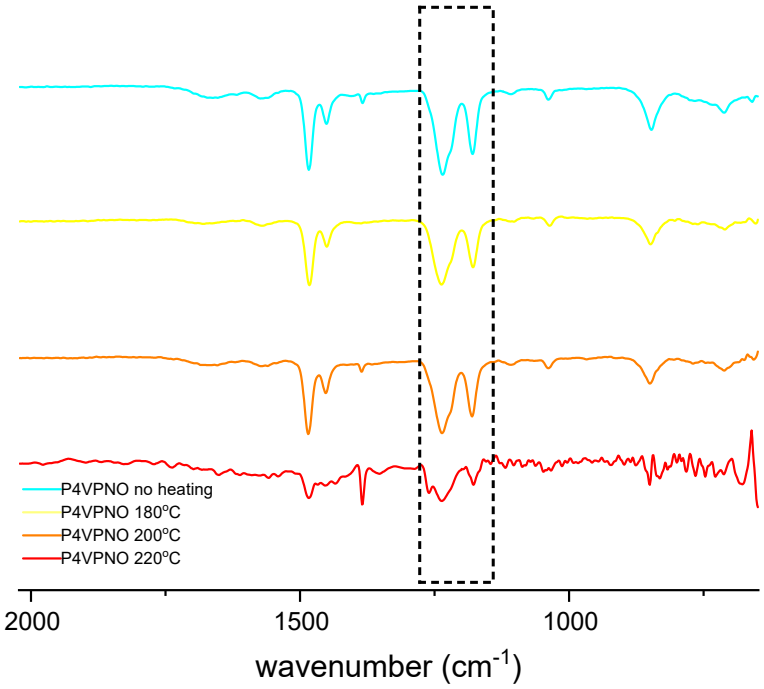

Figure S22. ATR-FTIR data of the P4VPNO degradation study. The bands at 1180, 1230 cm^{-1} associated with the N^{+}-O^{-} bond are intact up to 200 °C, with partial distortion evident at 220 °C.

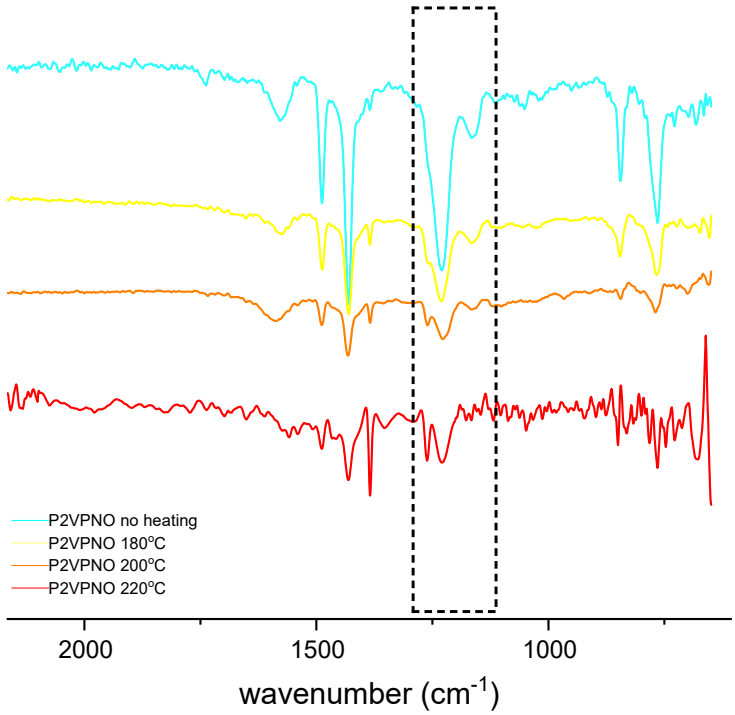

Figure S23. ATR-FTIR data of the P2VPNO degradation study. The bands at 1170, 1230 cm^{-1} associated with the N^{+}-O^{-} bond are intact up to 180 °C, with partial distortion evident at 200 °C.

Density Measurement by Pycnometry

A 2 ml glass pycnometer for precise volumetric measurements was used for the determination of the density of P2VPNO and P4VPNO homopolymers. The temperature was 21±1 °C. For the measurement P2VPNO or P4VPNO dried powder was compression molded for 10 minutes at 130°C inside a PTFE mold, to prepare several flat discs of the polymer. By applying high pressure with the hot press, we ensured that no visible air bubbles were entrapped in the polymer discs. The discs were removed from the PTFE mold and added to the pycnometer which was then filled with cyclohexane (d=0.774g/cm^3). The volume of the polymer was determined, and the density was measured as the average of multiple different homopolymer samples. For P4VPNO, samples with

molecular weights M_n=3.3K, 19.7K, 36.6K, 42.1K were measured. For P2VPNO, samples with molecular weights M_n=36.3K, 99.1K were measured two different times each.

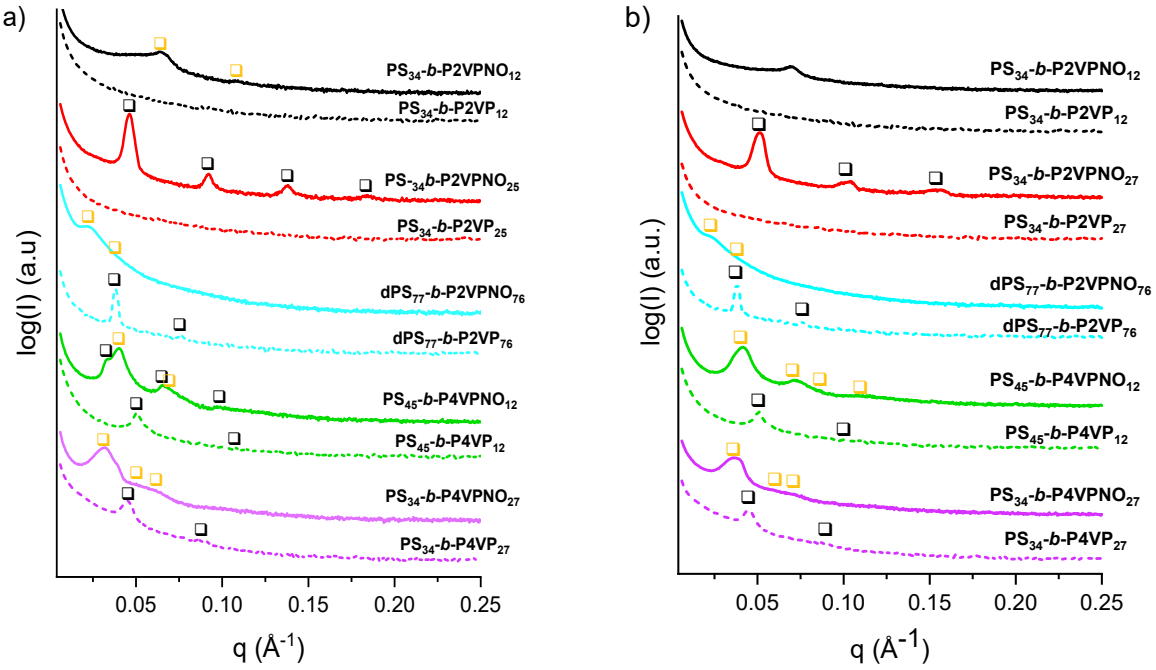

Figure S24. Room Temperature SAXS spectra of precursor PS-*b*-P2VP, dPS-*b*-P2VP or PS-*b*-P4VP block copolymers (thermally annealed) and oxidized PS-*b*-P2VPNO, dPS-*b*-P2VPNO or PS-*b*-P4VPNO block copolymers annealed with a) SVA, or b) a two-step (SVA and thermal annealing) process. The black arrows refer to scattering peaks in the sequence of 1:2:3:4 indicative of lamellar structures, while the orange arrows refer to scattering peaks in the

sequence of 1:√3:2 indicative of cylindrical structures.

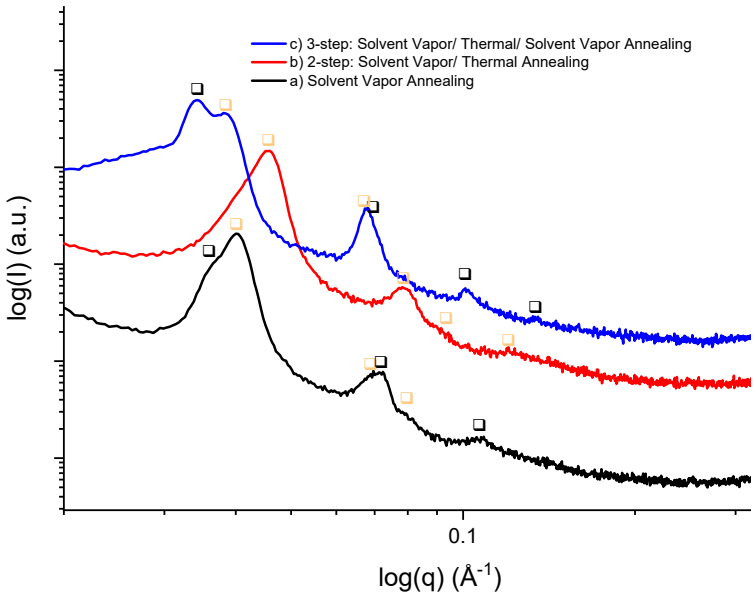

Figure S25. Room Temperature SAXS profiles of PS_{45}-*b*-$P4VPNO_{12}$ after a) Solvent Vapor Annealing, b) Solvent Vapor Annealing with subsequent Thermal Annealing, c) Solvent Vapor Annealing with subsequent Thermal Annealing and final Solvent Vapor Annealing. The co-existence of lamellar and cylindrical morphologies after the Solvent Vapor Annealing at steps (a) and (c) is evident. The black arrows refer to lamellar structures, while the orange arrows refer to cylindrical structures.

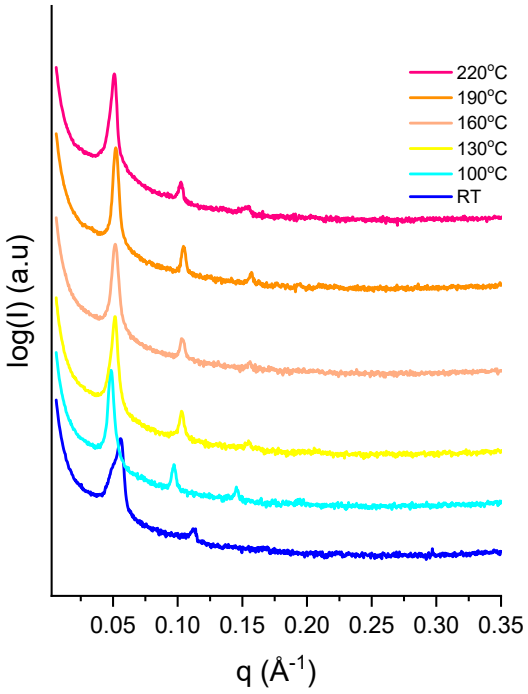

Figure S26. Temperature-dependent SAXS for PS_{34}-*b*-$P2VPNO_{25}$ after a Solvent Vapor Annealing and a subsequent thermal annealing step.

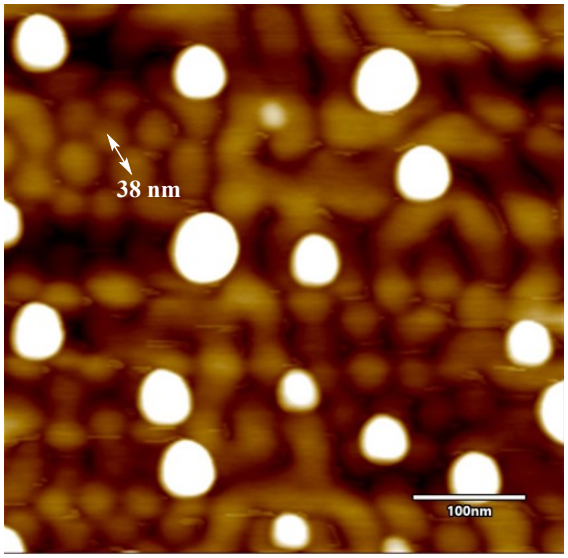
38 nm
100nm

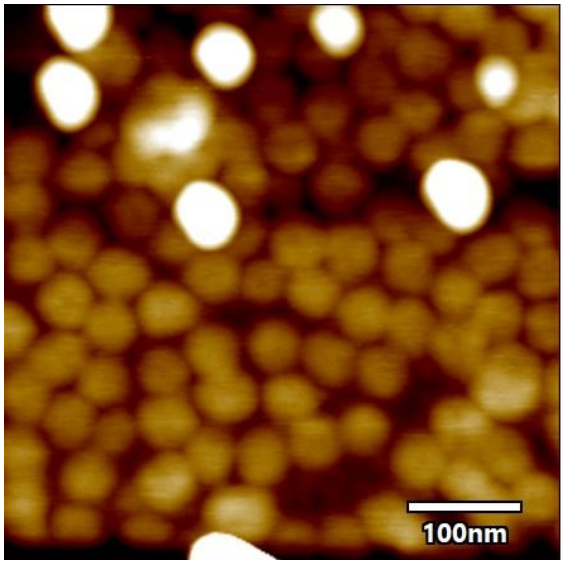
100nm

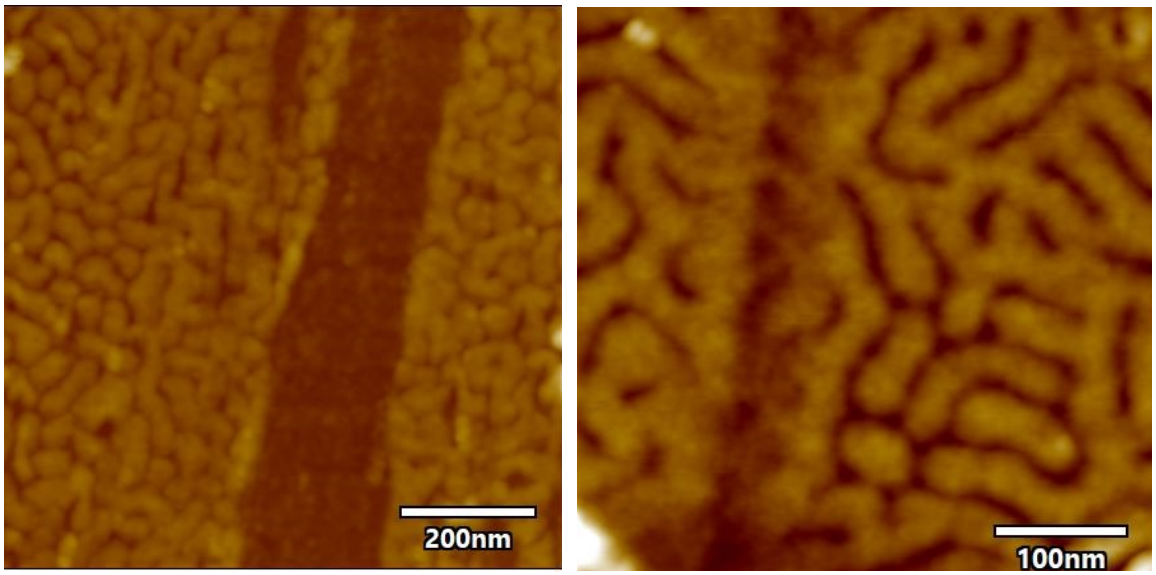

Figure S27. AFM images of HCP cylinders with mixed orientations (parallel and normal to the substrate).

References:

1 D. Uhrig and J. W. Mays, *J. Polym. Sci. Part A Polym. Chem.*, 2005, **43**, 6179–6222.

2 N. Hadjichristidis, H. Iatrou, S. Pispas and M. Pitsikalis, *J. Polym. Sci. Part A Polym. Chem.*, 2000, **38**, 3211–3234.

3 C. Sinturel, F. S. Bates and M. A. Hillmyer, *ACS Macro Lett.*, 2015, **4**, 1044–1050.

4 P. P. Angelopoulou, I. Moutsios, G. M. Manesi, D. A. Ivanov, G. Sakellariou and A. Avgeropoulos, *Prog. Polym. Sci.*, 2022, 135, 101625.

5 K. Azuma, J. Sun, Y. Choo, Y. Rokhlenko, J. H. Dwyer, B. Schweitzer, T. Hayakawa, C. O. Osuji and P. Gopalan, *Macromolecules*, 2018, **51**, 6460–6467.

6 J. G. Kennemur, *Macromolecules*, 2019, 52, 1354–1370.

7 A. Clark, M. Rosenbaum, Y. Biswas, A. Asatekin and P. Cebe, *Polymer (Guildf).*, 2022, **256**, 125176.

8 C. M. Lee, E. M. Pearce and T. K. Kwei, *Polymer (Guildf).*, 1996, **37**, 4283–4288.